Geochemistry Geophysics Geosystems G³
AN ELECTRONIC JOURNAL OF THE EARTH SCIENCES
Published by AGU and the Geochemical Society

Article
Volume 9, Number 2
8 February 2008
Q02S02, doi:10.1029/2007GC001791
ISSN: 1525-2027

Pacific offshore record of plinian arc volcanism in Central America: 2. Tephra volumes and erupted masses

S. Kutterolf
SFB574 at Kiel University/IFM-GEOMAR, Wischhofstrasse 1-3, D-24148 Kiel, Germany (skutterolf@ifm-geomar.de)

A. Freundt
SFB574 at Kiel University/IFM-GEOMAR, Wischhofstrasse 1-3, D-24148 Kiel, Germany

IFM-GEOMAR, Wischhofstrasse 1-3, D-24148 Kiel, Germany

W. Peréz
SFB574 at Kiel University/IFM-GEOMAR, Wischhofstrasse 1-3, D-24148 Kiel, Germany

[1] Sediment gravity cores collected from the Pacific seafloor offshore Central America contain numerous distal ash layers from plinian-type eruptions at the Central American Volcanic Arc dating back to more than 200 ka. In part 1 of this contribution we have correlated many of those ash layers between cores and with 26 tephras on land. The marine ash layers cover areas of up to 10^6 km^2 in the Pacific Ocean and represent a major fraction (60–90%) of the erupted tephra volumes because the Pacific coast lies within a few tens of kilometers downwind from the volcanic arc. Combining our own mapping efforts on land and published mapping results with our marine data yields erupted volumes of all major tephras along the arc that range from $\sim$1 to 420 km^3. Recalculated to erupted magma mass, the widespread tephras account for 65% of the total magma output at the arc. Complementing our tephra data with published volumes of the arc volcanic edifices and volcano ages, we calculate the long-term average magma eruption rates for each volcano. Moreover, we use incompatible element variations to calculate the cumulate masses that were fractionated during variable degrees of differentiation. This yields a minimum estimate of long-term average magma production rate at each volcano, because intrusives without surface expression and losses by erosion are not accounted for. Peak magma production rates increase from Costa Rica to Guatemala, but there is considerable scatter within each region and large differences even between neighboring volcanoes.

Components: 11,148 words, 6 figures, 2 tables.

Keywords: plinian volcanism; distal tephra distribution; magma production.

Index Terms: 8455 Volcanology: Tephrochronology (1145); 8428 Volcanology: Explosive volcanism; 8404 Volcanology: Volcanoclastic deposits.

Received 15 August 2007; **Revised** 11 October 2007; **Accepted** 23 October 2007; **Published** 8 February 2008.

Kutterolf, S., A. Freundt, and W. Peréz (2008), Pacific offshore record of plinian arc volcanism in Central America: 2. Tephra volumes and erupted masses, *Geochem. Geophys. Geosyst.*, *9*, Q02S02, doi:10.1029/2007GC001791.

Theme: Central American Subduction System
Guest Editors: G. Alvarado, K. Hoernle, and E. Silver

1. Introduction

[2] Ash plumes of numerous plinian, phreatoplinian and ignimbrite-forming eruptions from calderas and stratocones along the Central American Volcanic Arc (CAVA) were dispersed westward across the Pacific at stratospheric heights [*Kutterolf et al.*, 2007a, 2008]. The resulting marine ash layers cover areas of up to 10^6 km^2 in the Pacific Ocean (Figure 1) and represent a major fraction of the erupted tephra volumes because the CAVA volcanoes lie within a few tens of kilometers east of the Pacific coast (Figure 1).

[3] In part 1 we used our database of bulk-rock, glass and mineral major and trace element compositions, petrographic and lithologic characteristics, and eruption ages of all plinian and comparatively large, Pleistocene to recent tephras of the CAVA from Costa Rica to Guatemala to correlate ash layers in the Pacific seafloor with 26 tephras on land and thereby obtained a tephrostratigraphic framework for 1100 km length of the CAVA [*Kutterolf et al.*, 2008]. In this second part of our contribution, we use these correlations, our mapping results on land, and published isopach maps to better constrain erupted volumes of the widespread tephras and thus the magnitudes of the large eruptions that occurred at the CAVA during the past 200 ka.

[4] A fundamental problem with subduction zones is the budgeting of material input versus material output. The most significant output is the flux of magma through the volcanic arc, because this also largely determines the associated output fluxes of water and other volatiles. Previous attempts to determine magma fluxes at the CAVA considered magma masses stored in the volcanic edifices. Here we improve such estimates by including the magma masses represented by the widespread tephras which, as will be shown below, constitute a large part of the total magma output.

2. Geological Setting

[5] The Central American Volcanic Arc (CAVA) extends from Panama to Guatemala and runs roughly parallel to, and 150–200 km away from, the deep-sea trench. This middle America trench results from the subduction of the Cocos plate beneath the Caribbean plate at a convergence rate of 70–90 mm/a [*Barckhausen et al.*, 2001; *DeMets*, 2001]. The volcanic arc resulting from this subduction is one of the most active arcs on Earth and produced numerous plinian eruptions in the last several hundred thousand years. Easterly winds prevailing in the lower stratosphere distributed the ash across the Pacific Ocean where resulting ash layers provide marker beds in the mostly non-erosive submarine environment.

[6] The observations of numerous active bend faults across the outer rise of the Cocos plate penetrating the crust and uppermost mantle [*Ranero et al.*, 2003], and the anomalous heat flow and seismic velocities indicative of substantial hydration by seawater invading the faults [*Grevemeyer et al.*, 2005], suggest hydrated crust and serpentinized mantle as major carriers of water that ultimately drives melting in the mantle wedge and arc volcanism [*Rüpke et al.*, 2002]. The volcanic front in Nicaragua shifted to its present position about 8 Ma ago probably in response to re-arrangement of the subduction angles [*Barckhausen et al.*, 2001; *DeMets*, 2001; *Ehrenborg*, 1996] whereas it has had a more or less stable position in Costa Rica and Guatemala. The arc is tectonically segmented by Caribbean tectonic structures as well as by strike-slip tectonics caused by slightly oblique subduction [*DeMets*, 2001; *Ranero et al.*, 2005]. Slab dip varies between 40° and 75° along the subduction zone [*Cruciani et al.*, 2005; *Protti et al.*, 1995; *Syracuse and Abers*, 2006].

[7] Variations in the nature of the incoming plate [*Hoernle et al.*, 2002], in crustal thickness and composition [*Carr*, 1984] and the tectonic setting, are paralleled by along-arc variations in the composition of the volcanic rocks [*Carr et al.*, 2003, 2007a; *Carr*, 1984; *Feigenson and Carr*, 1986; *Feigenson et al.*, 2004; *Hoernle et al.*, 2002; *Patino et al.*, 1997, 2000] and the magnitudes of eruptions [*Rose et al.*, 1999]. In addition, variable degrees of magmatic differentiation led to compositions ranging from basalt through rhyolite. Such

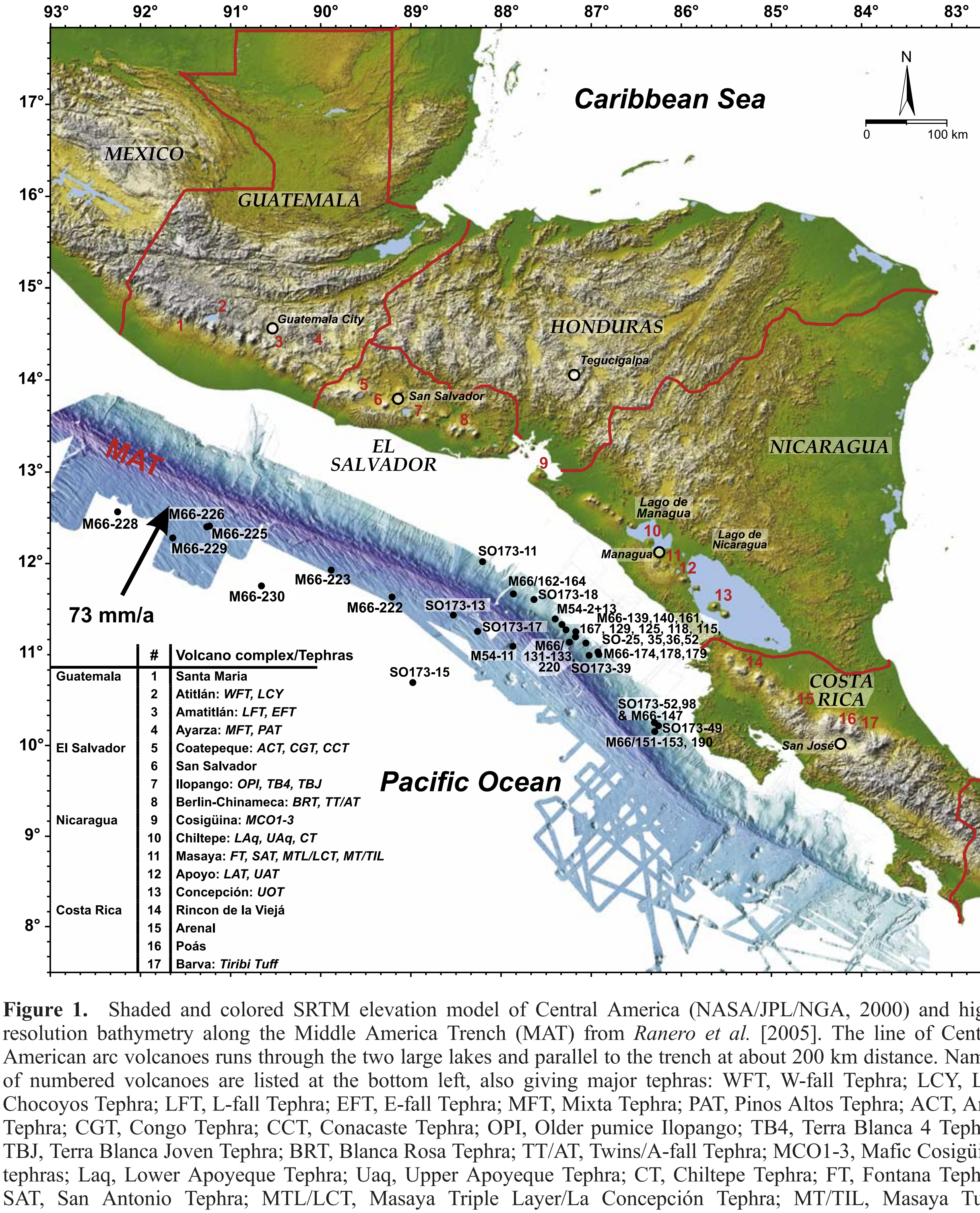

Figure 1. Shaded and colored SRTM elevation model of Central America (NASA/JPL/NGA, 2000) and high-resolution bathymetry along the Middle America Trench (MAT) from *Ranero et al.* [2005]. The line of Central American arc volcanoes runs through the two large lakes and parallel to the trench at about 200 km distance. Names of numbered volcanoes are listed at the bottom left, also giving major tephras: WFT, W-fall Tephra; LCY, Los Chocoyos Tephra; LFT, L-fall Tephra; EFT, E-fall Tephra; MFT, Mixta Tephra; PAT, Pinos Altos Tephra; ACT, Arce Tephra; CGT, Congo Tephra; CCT, Conacaste Tephra; OPI, Older pumice Ilopango; TB4, Terra Blanca 4 Tephra; TBJ, Terra Blanca Joven Tephra; BRT, Blanca Rosa Tephra; TT/AT, Twins/A-fall Tephra; MCO1-3, Mafic Cosigüina tephras; Laq, Lower Apoyeque Tephra; Uaq, Upper Apoyeque Tephra; CT, Chiltepe Tephra; FT, Fontana Tephra; SAT, San Antonio Tephra; MTL/LCT, Masaya Triple Layer/La Concepción Tephra; MT/TIL, Masaya Tuff/ Ticuantepe Lapilli; LAT, Lower Apoyo Tephra; UAT, Upper Apoyo Tephra; UOT, Upper Ometepe Tephra. Dots show core positions of R/V *METEOR* cruises M66/3a + b and M54/2 and R/V *SONNE* cruise SO173/3 along and across the trench.

compositional variations greatly assisted the geochemical correlations with marine ash beds presented in part 1 [*Kutterolf et al.*, 2008].

3. CAVA Tephrostratigraphy

[8] A number of publications have investigated tephrostratigraphic successions in middle to northern Central America [e.g., *Commision Ejecutiva Hidroelectrica del Rio Lempa* [CEL] 1992; *CEL*, 1995; *Drexler et al.*, 1980; *Freundt et al.*, 2006; *Hart*, 1983; *Koch and McLean*, 1975; *Kutterolf et al.*, 2007b; *Newhall*, 1987; *Pérez and Freundt*, 2006; *Peterson and Rose*, 1985; *Pullinger*, 1998; *Rose*, 1987; *Rose et al.*, 1999; *Wehrmann et al.*, 2006; *Wundermann and Rose*, 1984, *Scott et al.*, 2006; *Self et al.*, 1989].

[9] As described in part 1, we have used these studies to collect samples for our compositional data-base in Central America, and extended earlier studies in El Salvador and Nicaragua by own mapping and stratigraphic work in collaboration with the local geological services (SNET, San Salvador; INETER, Managua; INSIVUMEH, Guatemala City).

[10] Upper Pleistocene (since ~500 ka) to Holocene arc volcanism of Central America formed a number of large caldera volcanoes which produced large-magnitude eruptions of highly evolved, silicic magmas [*Rose et al.*, 1999]. Although large calderas are less common in Nicaragua and Costa Rica, volcanoes that generated major plinian eruptions were frequently active in Nicaragua since the Upper Pleistocene. Therefore the Pacific submarine sediment successions sampled offshore Central America contain ash layers from particularly large eruptions at the Ayarza, Amatitlán and Atitlán calderas in Guatemala, the Berlin-Chinameca complex, Ilopango Caldera, and Coatepeque Caldera in El Salvador and Apoyo Caldera, Masaya Caldera, Chiltepe volcanic complex, and Cosigüina volcano in Nicaragua (Figure 1). The cores offshore southern Nicaragua and Costa Rica show mostly ash layers from particularly large eruptions at Concepción volcano, as well as eruptions of Barva volcano in Costa Rica.

4. Methods

4.1. Marine Ash Layer Correlations

[11] During R/V *METEOR* cruises M54/2 and M66/3 as well as R/V *SONNE* cruise SO173/3, we collected 56 sediment gravity cores offshore Central America. These cores were located between 9°12′N/84°39′E and 12°15′N/91°30′E on the oceanic plate and the continental slope, at distances of 150–530 km from the CAVA (Figure 1). The cores contain 213 ash horizons including primary ash layers and slightly reworked ash that retained its compositional integrity and stratigraphic position. Criteria identifying primary and variably reworked ash horizons, and the methods employed to correlate them with deposits on land are described and discussed in part 1 [*Kutterolf et al.*, 2008].

4.2. Tephra Distribution, Volumes, and Masses

[12] To construct the isopach maps of the tephra layers onshore, we logged ~100 outcrops in El Salvador and Guatemala to complement thickness data from earlier studies [*CEL*, 1992, 1995; *Rose et al.*, 1987; *Wundermann*, 1982; *Wundermann and Rose*, 1984] (Figure 2). We also include unpublished thickness data collected and kindly provided by Carlos Pullinger, Dolors Ferres and Walter Hernandez of the Servicio Nacional de Estudios Territoriales (SNET) in El Salvador. In west-central Nicaragua, we have revised and extended earlier work by *Bice* [1985], identified and dated tephras not previously recognized, and constructed isopach and isopleth maps of all these deposits [*Freundt et al.*, 2006; *Kutterolf et al.*, 2007b; *Pérez and Freundt*, 2006; *Wehrmann et al.*, 2006].

[13] Here we further extend land-based results by including the offshore data. Since the offshore thickness data is sparse, the shape of the distal isopachs can only be estimated and introduces some error into the volume calculations. Total tephra volumes are obtained by fitting straight lines to data on plots of ln [isopach thickness] versus square root [isopach area] following *Pyle* [1989] and *Fierstein and Nathenson* [1992] and integrating to infinity. In most cases, the data required two straight-line segments to fit proximal to medial and distal data separately. We use the point of intersection of these line segments to distinguish between the volume contributions from proximal to medial and distal facies.

[14] We also use different approaches to convert tephra volume to magma mass over proximal to medial and distal regions. The proximal to medial volume of each tephra was reduced by 50% to account for interparticle pore space (space between pumice clasts) and lithic contents. Measured bulk densities of pumice and scoria lapilli range from

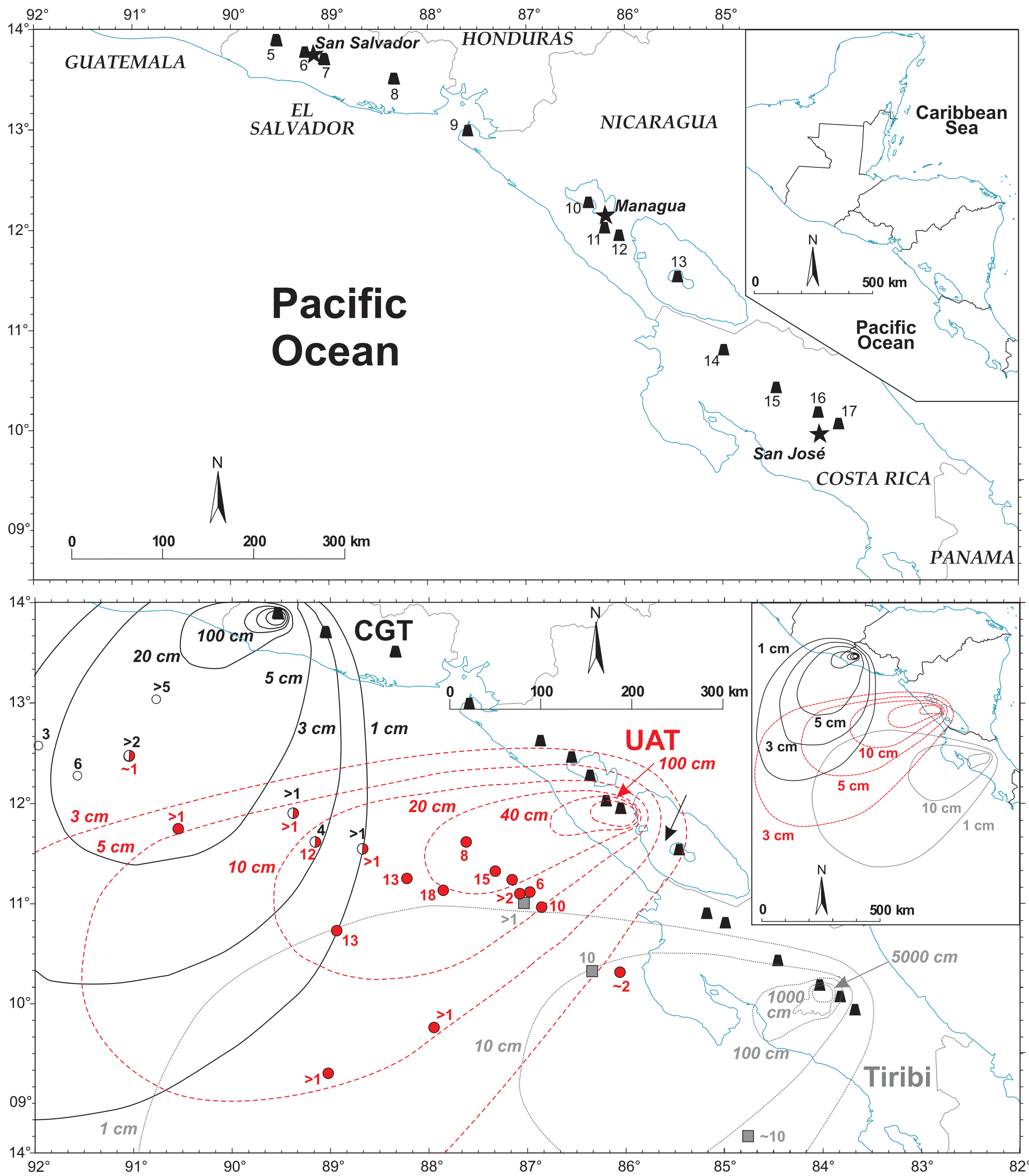

Figure 2. Selected isopach maps for the Tiribi Tuff, Upper Apoyo Tephra (UAT), and Congo Tephra (CGT), with isopachs on land taken from the references mentioned in the text. For clarity, we do not distinguish between well-constrained and poorly constrained isopach sections but note that the pattern of offshore isopachs is constrained by a few available data only. Isopach maps of every correlated tephra can be found in auxiliary material Figure S1.

400 to 810 kg/m^3 [e.g., *Kutterolf et al.*, 2007b], depending on composition. We used average values of 600 kg/m^3 for felsic and 800 kg/m^3 for mafic tephras to convert the remaining volume to magma mass.

[15] In the distal, marine region primary ash layers have a sharp base but gradually change into mixtures of ash and pelagic sediment at the top. From analyses of such mixed sediments we conclude that, on average, 20% should be added to the primary ash layer thickness. Balancing this with the interparticle space (space between glass shards filled with water; measured average of ~40%) to be subtracted, we have reduced distal tephra volumes by an average of ~30% (25–35% per tephra). Measured average ash-particle densities of 2100 kg/m^3 for felsic and 2400 kg/m^3 for mafic

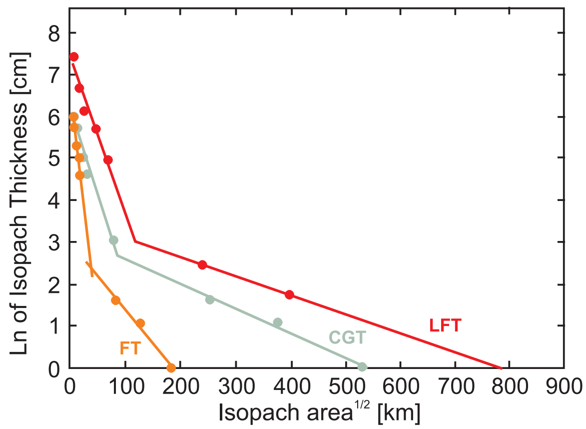

Figure 3. Natural logarithm of isopach thickness versus square root of isopach area for three selected tephras: Fontana tephra (FT), Congo Tephra (CGT), and L-fall Tephra (LFT). For all other mapped tephras, see auxiliary material Figure S2. As in the examples, most tephra data can be fitted by two line segments.

marine tephras are used to convert distal volumes to magma masses.

5. Tephra Volumes and Magma Masses

[16] Selected isopach maps and ln (thickness) versus square root (isopach area) variations are shown in Figures 2 and 3. The respective figures, Figures S1 and S2, for the remaining tephras are available as auxiliary material.[1] Single tephra volumes are summarized in Table 1 and are shown schematically along the CAVA in Figure 4, according age and regional distribution. Very fine ash from large eruptions is transported to much larger distances than investigated here and may even circle the globe. Such very distal deposits may produce a still shallower slope in ln (thickness) versus square root (isopach area) diagrams such that the volumes and masses we have determined are still minimum estimates. We now discuss every tephra according to the source volcanic centers in geographic order from north to south, using the correlations to marine ash layers established in part 1 [*Kutterolf et al.*, 2008].

5.1. Atitlán Caldera

[17] Atitlán Caldera is the source of an at least 200 ka old tephra succession comprising from old to young W-fall and flow tephra, Los Chocoyos H-fall and flow tephra, D-fall deposits, F-fall deposits, and I-fall deposits [*Rose et al.*, 1987]. We recognized two of these tephras in the Pacific record. The W-tephra on land comprises fall and pyroclastic flow deposits extending across ~10,000 km^2 with an estimated volume of 12 km^3 tephra (9 km^3 fall, 3 km^3 flow) [*Rose et al.*, 1999]. Correlation of 4 cm thick marine tephra C22 and an ash layer in the near-by core RC-12-32 of *Bowles et al.* [1973] to the 158 ± 3 ka old W-tephra enlarges the minimum distribution area (up to 5 cm isopach) to 6x10^4 km^2 and the erupted tephra volume to ~23.3 km^3 or ~1.8x10^{13} kg magma mass, respectively (Figures 4, S1, and S2 and Table 1).

[18] The 84 ± 0.5 ka old Los Chocoyos eruption produced the largest known Quaternary tephra in Central America with a tephra volume of 420 km^3 (200 km^3 flow and 220 km^3 fall), i.e., 280 km^3 DRE, that covers an minimum area of ~6 × 10^6 km^2 extending from the Pacific to the Gulf of Mexico [e.g., *Drexler et al.*, 1980; *Rose et al.*, 1987, 1999]. Our new data of correlated ash layer C21 to Los Chocoyos tephra confirms, but does not extend, these estimates and emphasizes the usefulness of this layer as a marker bed across the whole region (Figure 4 and Table 1).

5.2. Amatitlán Caldera

[19] Amatitlán Caldera is the source of at least six tephras which are from bottom to top the L-flow and fall, Z-falls, T-flow and fall, C-fall, E-fall and J-falls [*Koch and McLean*, 1975; *Wundermann*, 1982; *Wundermann and Rose*, 1984]. L-tephra is found in our marine cores as correlated ash layer C23 and, using documented compositional data, also in DSDP Leg 67 as well as in cores of *Bowles et al.* [1973]. The 191 ± 11 ka old L-tephra on land [*Rose et al.*, 1999] has a total tephra volume of 30–40 km^3 estimated by *Wundermann and Rose* [1984] and includes 12 km^3 DRE pyroclastic flow and 6 km^3 DRE fall deposits. It is spread out over an area of 1600 km^2. With the marine addition, we now estimate a minimum distribution area 7 × 10^5 km^2 (up to 2 cm isopach), corresponding to a tephra volume of 63.2 km^3 and a magma mass of 7.5 × 10^{13} kg including the flow volume (Figures 4, S1, and S2 and Table 1). Correlation of 119 ka old T-Fall Tephra to ash layers in DSDP core (Leg 66/493B-1-3) lead also to very rough estimates of ~17 km^3 and corresponding magma mass of ~3.7 × 10^{13} kg.

[1]Auxiliary material data sets are available at ftp://ftp.agu.org/apend/gc/2007gc001791. Other auxiliary material files are in the HTML.

Table 1. Summary of Correlated Tephras With Core Positions, Ages, Maximum Distance to Source, and Volume Estimations of Investigated Fallout Tephras

Tephra	Age[a]	Correlation Number	Distance to Source, km	Proximal Tephra Fallout Volume, km^3	Distal Tephra Volume, km^3	Total Fallout Tephra Volume, km^3	Estimated Flow Volumes After Literature	Approx. Total Magma Mass, 10^{13} kg
TBJ	1.6 ka; *D*	C1	390	32	38,6	70,6	(na)	6.6
MT/TIL	1.8 ka; *S*	C2	200	4.8	1.8	6.6	–	0.5
CT	1.9 ka; *S*	C3	570	3.9	14	17.9	–	2.2
MTL/LCT	2.1 ka; *D*	C4	170	0.8	2.6	3.4	–	0.5
SAT	6 ka; *S*	C5	330	0.5	13	13.5	–	2.2
Uaq	12.4 ka; *D*	C6	300	2.2	2.1	4.3	–	0.4
LAq	17 ka; *S*	C7	210	0.8^{+}	3,1	3.9	–	0.5
UOT	19 ka; *S*	C8	280	2.9^{+}	2.3	5.2	–	0.4
MCO	21–23 ka; *S*	C9	220	1.5^{+}	4.5	6	–	0.4
UAT	24.5 ka; *D*	C10	530	7.2	35.7	42.9	8	$7.2^{(y)}$
LAT	25 ka; *D*	C11	270	3	3.5	6.5	–	0.6
PAT	23 ka; *D*		460	$—^{(+)}$	$—^{(+)}$	$2^{(\#)}$	–	0.3
TB4	~36 ka; *S(228) CGT*	C12	380	25,9	10,4	36,3	–	2.3
MFT	*39 ka after S(228) CGT*	C13	940	2,9	6,1	9	–	1
CCT	~51 ka; *S(228)*	C14	320	$—^{(+)}$	$—^{(+)}$	11,2	1	0.3
EFT	51 ka; *S (D-3; Bowles)*		860	5	40	45	–	6
CGT	~53 ka; *D*	C15	320	$5.5^{(+)}$	$12.6^{(+)}$	18.1	5	~2
FT	60 ka; *S*	C16	330	1.3	1.4	2.7	–	0.3
TT/AT	60 ka; *S(222)*	C17	270	1	9.4	10.4	–	1.4
ACT	75 ka; *D*	C18	320	9.6	6.6	16.2	10	1.3
BRT	75 ka; *D*	C19	200	1.9	2.7	4.6	2	0.7
OPI	75–84 ka; *S*	C20	470	(na)	(na)	(na)	(na)	(na)
LCY	84 ka; *D*	C21	1900	(na)	(na)	$420^{(*)}$	200	$59^{(*)}$
TFT	119 ka; *D*		940	$\sim 8^{(X)}$	9	(na)	17	3.7
WFT	158 ka; *D*	C22	560	13.6	9.7	23.3	3	1.8
LFT	191 ka; *D*	C23	810	18.5	44.7	63.2	12	7.5
Tiribi	322 ka; *D*		230	$35^{(2)}$	42	78		2.2

[a] D, dating field tephra; S, dating from sedimentation rates.

[20] The E-tephra is a coarse grained reversely graded fall of white pumice clasts distributed across an area of ~1300km^2 on land, corresponding to a tephra volume of >5 km^3 (2.5 km^3 DRE) [*Wundermann*, 1982; *Wundermann and Rose*, 1984]. Correlations based on published data of an ash layer at DSDP Leg 84 (570-2-3), the D3 ash layer of *Bowles et al.* [1973] as well as the Y5 ash layer in the Gulf of Mexico documented by *Rabek et al.* [1985], which all have the E-tephra glass composition [*Kutterolf et al.*, 2008], yield a minimum distribution area (up to 1 cm isopach) of 6.3 × 10^5 km^2 (Figure S1), corresponding to a tephra volume of 45 km^3 (Figures 4 and S2 and Table 1; 6 × 10^{13} kg magma mass).

5.3. Ayarza Caldera

[21] Two nested calderas characterize the Ayarza Caldera in the south of Guatemala and produced the 27 ± 1.6 ka old Mixta Tephra, the Pinos Altos Tephra, and the younger (23 ±0.5 ka) Tapalapa Tephra [*Peterson and Rose*, 1985] (Table 1). The Mixta Tephra is a compositionally zoned tephra with pale brown to black and banded pumice clasts. Outcrops limited to near the source poorly constrain a volume of 0.1 km^3 DRE [*Peterson and Rose*, 1985]. Correlation to ash layer C12 in our core M66/3-228, to glass composition data of the C-layer of *Bowles et al.* [1973] reported by *Drexler et al.* [1980] as well as to glass composition data from DSDP Leg 84 (570-2-1/141) of an ash layer at 621 cm bsf, yield a new minimum distribution (up to 1 cm isopach) of 1.3 × 10^5 km^2 (Figure S1) and a tephra volume of ~9 km^3 (Figures 2, 4, and S2 and Table 1), which corresponds to 9.9 × 10^{12} kg erupted magma mass for the Mixta Tephra.

[22] The Pinos Altos Tephra is a thick pumice fall deposit, and *Peterson and Rose* [1985] estimated the erupted volume as at least 2 km^3 DRE on the basis of its identification at two distal sites on land and in marine core RC12-32 from the Pacific Ocean. Our trace element data confirm the corre-

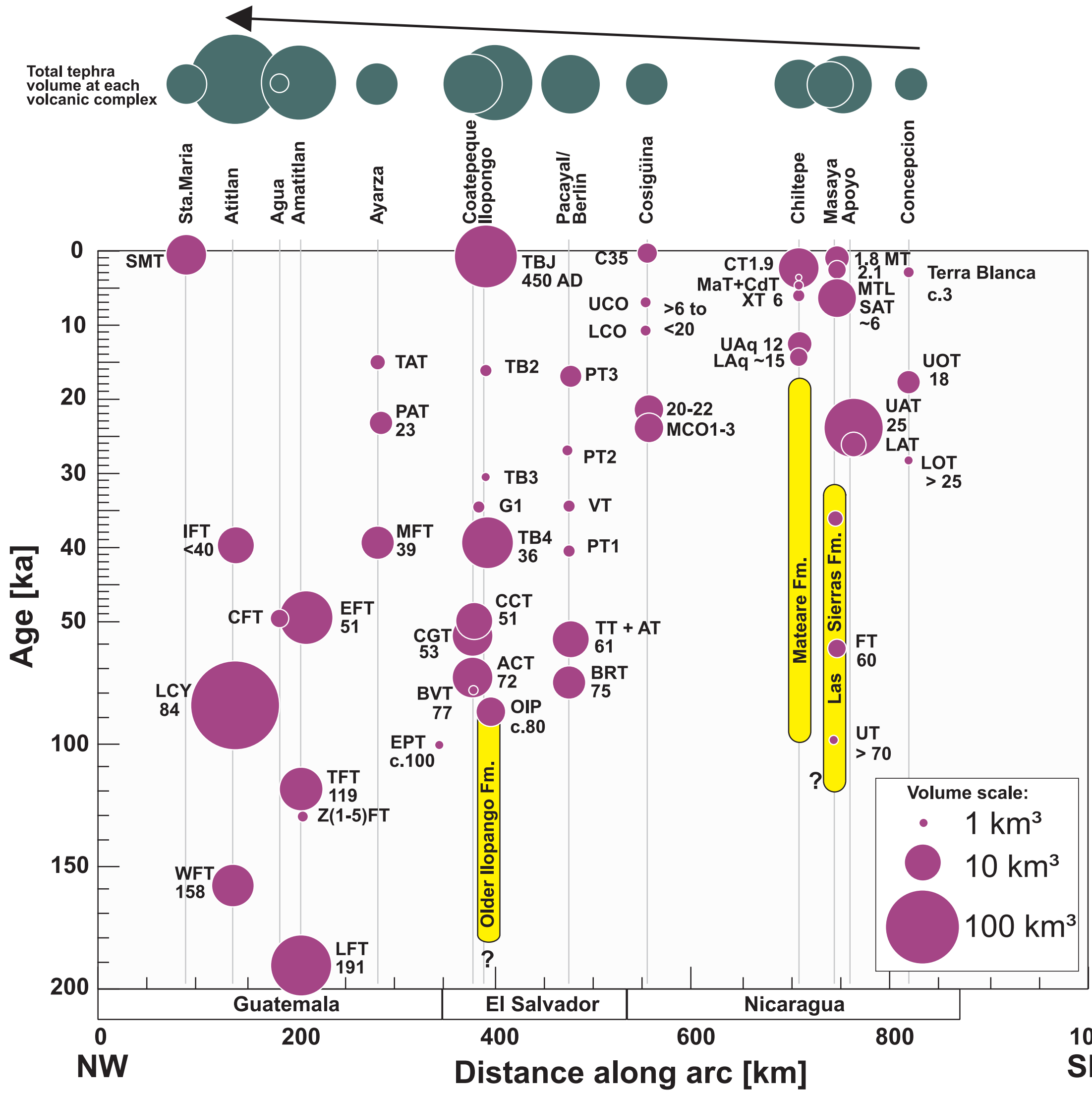

Figure 4. Composite tephrostratigraphy of Central America showing the position of source volcanoes along the arc versus age of tephras as in *Kutterolf et al.* [2008] but with violet symbol size scaled to erupted volume (diameter of volume-scaled sphere). Numbers next to each circle give the age of the tephra. See Figure 1 for acronyms. Green circles above each volcanic center represent the cumulative tephra volumes, the arrow indicating an increase northward.

lation with an ash layer 50 cm bsf in core RC12-32 of *Bowles et al.* [1973] but we did not find Pinos Altos Tephra in our cores.

5.4. Coatepeque Caldera

[23] A tephra succession of four widespread tephras can be found at Coatepeque Caldera in northern El Salvador starting with the Bellavista eruption at 77 ± 2 ka [*Rose et al.*, 1999] and followed by the 72 ± 3 ka old Arce Tephra, the Congo Tephra (53 ± 3 ka; own radiocarbon dating) and the ~51 ka old Conacaste Tephra. The Arce tephra is the largest of the four Coatepeque tephras and includes plinian fall beds and ignimbrite. Mapping for a geothermal reconnaissance project [*CEL*, 1992] yielded a distribution area of 2000 km^2 and a total tephra volume of ~40 km^3 (17 km^3 DRE). Correlation to ash layer C18 in our cores gives the new minimum distribution area (up to 2 cm isopach) of 1×10^5 km^2, and the minimum tephra fall volume is 16.2 km^3 (~1.3×10^{13} kg magma mass) (Figures 4, S1, and S2 and Table 1) to which the volume of the ignimbrite (>10 km^3), which we continue to map, must be added. Compositional data of ash beds sampled in the Caribbean by *Rabek et al.* [1985] (K131-446 cm bsf; TR126-22

321 cm bsf) suggests that these are also distal Arce Tephra but we presently cannot validate this correlation with certainty. If these correlations were true, the Arce tephra volume would be ~70 km^3.

[24] The Congo Tephra is a complex succession of plinian fall, ignimbrite and surge deposits and reconnaissance studies of this tephra suggested a distribution area of ~900 km^2 and a tephra volume of ~15 km^3 (6 km^3 DRE [*CEL*, 1992]). We correlate ash layer C15 of our cores and an ash layer at DSDP Leg 84 [*Pouclet et al.*, 1985] with the Congo Tephra, which leads to 2.8×10^5 km^2 area of minimum distribution (up to 1 cm isopach; Figure 2) and a total tephra volume of 18.1 km^3, which corresponds to 2×10^{13} kg magma mass (Figures 3 and 4 and Table 1). Again, the volume of the ignimbrite and surge deposits, which we continue to map, has to be added to this fall volume.

[25] The newly described Conacaste Tephra comprises a lower fall section of two pumice lapilli beds bracketing a central fine ash fall extremely rich in accretionary lapilli, and an upper surge package, which were produced by a phreatoplinian eruption. Ash layer C14 in our cores can be correlated to Conacaste Tephra. We still need to map the Conacaste Tephra in more detail; preliminary estimates including the offshore data suggest a minimum distribution (up to 1 cm isopach) of 6×10^4 km^2 and a tephra volume of 11.2 km^3 corresponding to 3.4×10^{12} kg magma mass (Figures 4, S1, and S2 and Table 1).

5.5. Ilopango Caldera

[26] At least five tephra deposits were produced by the central El Salvadorian Ilopango caldera since the Upper Pleistocene. From youngest to oldest, these are the Tierra Blanca Joven (TBJ) and the TB2, TB3 and TB4 Tephras [*Rose et al.*, 1999]; in addition, there are remains of a deposit from an older eruption at the shore of the caldera lake [*Mann et al.*, 2004]. The A.D. 429 ± 107 old Terra Blanca Joven eruption (TBJ) [*Dull et al.*, 2001] comprises a succession of fall, ignimbrite and surge deposits [*Hart and Steen-McIntyre*, 1983]. These authors estimated a distribution area of 10,000 km^2 and a volume of 18 km^3 DRE. The TBJ Tephra can be correlated to ash layer C1 in the upper few decimeters of our Pacific sediment cores and we also recognized it in the core data of *Bowles et al.* [1973]. Combining the onshore and offshore thickness data we obtain a tephra volume of 70.6 km^3, which corresponds to a magma mass of 6.6×10^{13} kg that is distributed across an minimum area minimum (up to 3 cm isopach) of 3×10^5 km^2 (Figures 4, S1, and S2 and Table 1).

[27] The ~36 ka old TB4 Tephra is a prominent white massive pumice lapilli fall deposit widely distributed over El Salvador. We identified ash layer C12 in our cores and ash layers at DSDP Leg 67 as the distal equivalent of TB4. Using reconnaissance mapping on land by *CEL* [1992], unpublished data by SNET, and the marine data, the TB4 tephra volume becomes 36.3 km^3 (2.3×10^{13} kg magma mass; Table1 and Figures 4 and S2) distributed across an minimum area (up to 5 cm isopach) of 7×10^4 km^2 (Figure S1).

[28] Additionally we found a thin ash layer in core 226 which has the composition of the older pumice deposit inside Ilopango caldera described by *Mann et al.* [2004]. These two far-apart data points do not allow us to estimate the tephra volume but do demonstrate that this was another large eruption that occurred at Ilopango between 73–84 ka ago [*Kutterolf et al.*, 2008].

5.6. Berlin-Pacayal-Volcan Group

[29] Ian Nairn and coworkers of DSIR, New Zealand, performed a stratigraphic study of the volcanic deposits from this group of volcanoes in southern El Salvador [*CEL*, 1995] and identified six major tephras in the Upper Pleistocene succession. These are from old to young: the Blanca Rosa Tephra (75 ± 10 ka), Twins/A-Tephra (~61 ka), Pacayal 1 Tephra, Volcan Tephra and Pacayal 3 Tephra, but we only could correlate the Blanca Rosa and Twins/A-tephra to Pacific sediment cores. The Twins and A tephras have been previously described as three separate units but *Kutterolf et al.* [2008] interpret the three layers as the deposits of one eruption producing three thick fall lapilli beds as well as a pyroclastic flow deposit. Nairn and coworkers have estimated the areal distribution as 900 km^2 with a total tephra volume of 12 km^3 (~6 km^3 DRE). Since Layer C17 in our cores correlates to Twins/A-Tephra the minimum distribution area (up to 3 cm isopach) becomes 1×10^5 km^2 (Figure S1) and the tephra volume accounts for 10.4 km^3 (1.4×10^{13} kg magma mass; Table 1 and Figures 4 and S2).

[30] Additionally major element glass compositions suggest that an ash layer in core SO173/3-18 may correlate with the Blanca Rosa Tephra, which would lead to an minimum aerial distribution (up to 5 cm isopach) of 2.5×10^4 km^2 and a

total fall volume of 4.6 km^3, yielding 6.5 × 10^{12} kg magma mass, when proximal pyroclastic flow deposits are included (Figures 4, S1, and S2 and Table 1).

5.7. Cosigüina Caldera

[31] Cosigüina volcano at the northern end of the Nicaraguan volcanic arc produced several widespread tephras prior to the last plinian eruption in A.D. 1835 which is the only one studied [*Williams*, 1952; *Self et al.*, 1989; *Scott et al.*, 2006]. We sampled three mafic fall tephras (MCO1 to MCO3) and two overlying dacitic falls, the Lower and Upper Cosigüina tephras (LCO and UCO), but could correlate marine ashes only to the mafic falls. Ash layer C9 in our cores offshore Nicaragua and Southern Salvador correlate compositionally with the ~21 to 23 ka old MCO tephras. Using also compositional data of cores V-15-26 (510 and 539 cm bsf) and V-15-22 (112 cm bsf) documented by *Bowles et al.* [1973] extends the minimum distribution (up to 1 cm isopach) of those tephras 200 km to the west and 180 km to the south of Cosigüina volcano (6 × 10^4 km^2) but, due to the few available thickness data, only allows a very rough estimate of the tephra volume as around 6 km^3 (4 × 10^{12} kg magma mass) at least for the uppermost tephra MCO1 (Figure 4 and Table 1).

5.8. Chiltepe Volcanic Complex

[32] The Chiltepe volcanic complex includes Apoyeque stratocone, the Xiloa maar, at least two more, now hidden, vents of plinian eruptions and several basaltic cinder cones and maars [*Kutterolf et al.*, 2007b]. During the past 15 ka, six (phreato-)plinian dacitic tephras erupted from this area: the Lower (~17 ka) and Upper Apoyeque (12.4 ka) tephras, the 6.1 ka Xiloa Tephra, the Mateare and Los Cedros tephras, and finally the 1.9 ka old Chiltepe Tephra. In part 1 we have been able to correlate ash layer C3 in the pacific sediment cores and an ash layer 75 cm bsf in core V-15-26 of *Bowles et al.* [1973] to the Chiltepe Tephra. Considering these distal thickness data, the tephra volume of 4 km^3 estimated from on-land data by *Kutterolf et al.* [2007b] must now be increased to 17.9 km^3 corresponding to 2.2 × 10^{13} kg magma mass, distributed across an minimum area (up to 1 cm isopach) of 1.7 × 10^5 km^2 (Figures 4, S1, and S2 and Table 1).

[33] The 12.4 ka old, coarse grained, reversely graded Upper Apoyeque Tephra pumice fall is correlated to reworked ash pods (ash layer C6) and it probably correlates also with a >1-cm-thick ash layer 580 cm bsf in core V-15-26 of *Bowles et al.* [1973]. The minimum distribution area (up to 1 cm isopach) thus is 5 × 10^4 km^2 and the tephra volume of 4.3 km^3 corresponds to 3.7 × 10^{12} kg magma mass (Figures 4, S1, and S2 and Table 1).

[34] The Lower Apoyeque Tephra compositionally corresponds to ash layer C7, which allows a minimum estimate of 3.9 km^3 (Table 1 and Figures 4 and S2) of erupted tephra volume corresponding to 5.4 × 10^{12} kg magma mass distributed across an minimum area (up to 1 cm isopach) of 5 × 10^4 km^2 (Figure S1).

5.9. Masaya Caldera

[35] The Masaya Caldera is a volcano that has produced large-magnitude plinian and phreatomagmatic eruptions of mafic composition [*Bice*, 1980, 1985; *Williams*, 1983]. The Fontana Tephra (FT) is a layered sequence of scoria lapilli fall beds that have a wide, plinian dispersal and erupted from a vent northwest of the Masaya Caldera [*Wehrmann et al.*, 2006] about 60 ka ago [*Kutterolf et al.*, 2008]. Vents within Masaya Caldera erupted the plinian to phreatomagmatic San Antonio Tephra (SAT, ~6 ka), the Masaya Triple Layer/La Concepción Tephra (MTL/LCT; 2.1 ka), and finally the Masaya Tuff/Ticuantepe Lapilli (MT/TIL), the product of a huge surtseyan eruption 1.8 ka ago that ended in a plinian phase [*Kutterolf et al.*, 2007b; *Pérez and Freundt*, 2006]. Correlations of marine ash layer C2 to MT/TIL facilitate the extension from 2 × 10^3 km^2 to 4.3 × 10^4 km^2 minimum distribution area (up to 1 cm isopach) by including the distal data. This yield a new tephra volume of ~6.6 km^3 (~5 × 10^{12} kg magma mass; Table 1 and Figures 4, S1, and S2).

[36] The MTL/LCT plinian deposit onshore can be correlated to marine mafic ash layer C4 which leads to a minimum distribution area (up to 3 cm isopach) of 2.2 × 10^4 km^2 and new total tephra volume of 3.4 km^3 (~4.8 × 10^{12} kg magma mass; Table 1 and Figures 4, S1, and S2).

[37] The widespread San Antonio Tephra onshore (~8500 km^2) is a sequence of black scoria falls overlain by surge deposits. A tephra volume of ~0.5 km^3 has been estimated by *Pérez and Freundt* [2006]. Geochemical fingerprinting shows that marine ash layer C5 and additionally a >1-cm-thick ash layer 270 cm bsf in core V-15-26 of *Bowles et al.* [1973] is equivalent to the SAT. The corresponding new minimum distribution (up to

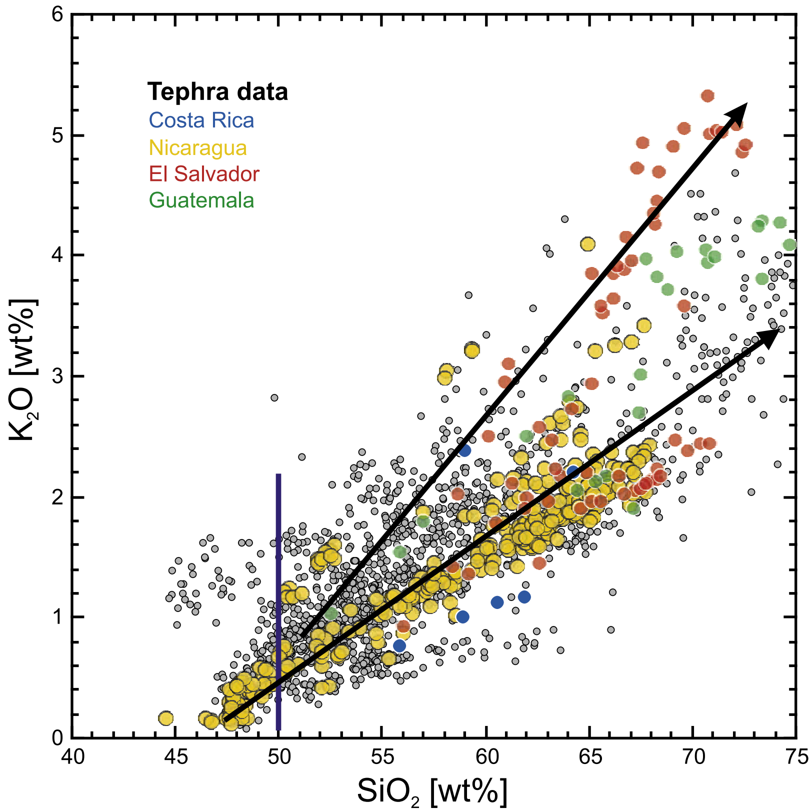

Figure 5. K_2O versus SiO_2 diagram showing the compositional range of the CAVA volcanic rocks from basalt through rhyolite due to different extents of fractional crystallization (XRF data from Carr et al. database; *Patino et al.* [2000] and *Carr et al.* [2003] (gray dots); and own data (colored dots)). Incompatible K_2O increases linearly to higher silica contents within magmatic series as indicated by the lines. Vertical blue line at SiO_2 = 50 wt% intersects K_2O contents used to determine fractionation factors.

3 cm isopach) is then 1.2×10^5 km^2 (Figure S1). The erupted tephra volume of 13.5 km^3 corresponds to 2.2×10^{13} kg magma mass for the San Antonio Tephra, which thus represents one of the biggest mafic eruptions in Central America since the Upper Pleistocene (Table 1 and Figures 4 and S2).

[38] The Fontana Tephra compositionally corresponds to marine ash layer C16 in the Pacific sediment cores. This allows a minimum estimate of 2.7 km^3 (Figures 4 and S1) of erupted tephra volume, which doubles the previous estimate by *Wehrmann et al.* [2006] and corresponds to 2.9×10^{12} kg magma mass distributed across an minimum area (up to 1 cm isopach) of 3.4×10^4 km^2 (Figure 3).

5.10. Apoyo Caldera

[39] Apoyo Caldera, in Central Western Nicaragua, generated two large plinian eruptions in rapid succession 24.5 ka ago, the Lower (LAT) and Upper (UAT) Apoyo tephras which are separated by an incipient paleosol [*Kutterolf et al.*, 2007b]. The LAT is a pumice fall deposit, the UAT also comprises coarse-grained pyroclastic surge deposits and about 8 km^3 of ignimbrite distributed mainly to the east of the caldera and into Lake Nicaragua [*Sussman*, 1985]. The UAT correlates with marine ash layer C10 as well as with ash beds in cores V-15-27, 18, 22 and 26 of *Bowles et al.* [1973] offshore Central America. The resulting UAT fall tephra volume is 42.9 km^3 (Table 1 and Figures 4 and S2) distributed across an minimum area (up to 3 cm isopach) of at least 3.7×10^5 km^2 (Figure 2). Including also the 8 km^3 proximal ignimbrite and its density of 2200 kg/m^3 estimated by *Sussman* [1985] gives an erupted magma mass of 7.2×10^{13} kg.

[40] The Lower Apoyo Tephra correlates with marine ash layer C11 which extends its minimum distribution (up to 1 cm isopach) across 5×10^4 km^2 (Figure S1) resulting in a total tephra volume

of 6.5 km^3 (~6 × 10^{12} kg magma mass; Table 1 and Figures 4 and S2).

5.11. Concepción Volcano

[41] Concepción on Ometepe island produced several basaltic to dacitic pyroclastic tephras [*Borgia and van Wyk de Vries*, 2003]. One of those, the ~19 ka old Upper Ometepe Tephra, is correlated to marine ash layer C8 offshore Nicaragua and can also be found in cores V-15-18, 27 and 19 of *Bowles et al.* [1973]. The resulting UOT minimum aerial distribution (up to 1 cm isopach) of 7 × 10^4 km^2 (Figure S1) and the tephra volume of 5.2 km^3 (~4.2 × 10^{12} kg magma mass; Table 1 and Figures 4 and S2) are mainly based on offshore data since exposure on land is poor.

5.12. Tiribi Tuff From Costa Rica

[42] The Tiribi Tuff, the largest Costa Rican eruption in the last 350 ka, has erupted from Barva volcano. Compared to other CAVA rocks, it has a unique chemical composition [*Pérez et al.*, 2006] which makes it easy to correlate with marine ash beds. We find the distal ash of the Tiribi Tuff in core M66/3a-147 and also as the I6-Layer of *Ledbetter* [1985]. *Peréz et al.* [2006] estimated a tephra volume of 35 km^3 DRE on the basis of land data, which is now increased to ~80 km^3 tephra volume (2,2 × 10^{13} kg magma mass; Figures 4 and S2 and Table 1) considering the offshore minimum distribution (up to 1 cm isopach) of 3.6 × 10^5 km^2 (Figure 2).

6. Erupted Masses and Mass Fluxes Along the CAVA

[43] Previously, erupted masses along the Central American volcanic arc have been calculated from the volumes of volcano edifices [*Carr*, 1984]. This approach has been revised by *Carr et al.* [1990, 2007b], who already calculated magma mass fluxes but without including the volumes of widespread tephras. We extend this approach by adding erupted masses of the widespread tephras to those volcanoes that produced them. Moreover, while average edifice compositions are basaltic to andesitic, tephras mostly have dacitic to rhyolitic compositions and we calculate the masses of fractionated cumulates trapped in the crust to estimate the total magma production for each volcano. Using the edifice volumes determined by *Carr et al.* [1990, 2007b], we calculated the corresponding magma masses using a density of 2800 kg/m^3 assuming that the edifice material is well compacted; this actually yields maximum estimates of the edifice magma masses while the tephra masses added tend to be minimum estimates.

[44] The wide compositional range of the CAVA volcanic rocks from basalt through rhyolite is largely due to different extents of fractional crystallization. Incompatible elements thus typically increase linearly to higher silica contents although the gradients vary between magmatic series. We use the variations of K_2O with silica (Figure 5) because this has been analyzed in all samples but other incompatible elements give similar results. Employing our own compositional data (Table S1) and that of Carr and coworkers [*Carr et al.*, 2003; *Patino et al.*, 2000] compiled at http://www.rci.rutgers.edu/~carr/, we determine an average ratio of observed K_2O content to the K_2O content at 50 wt% SiO_2 for each tephra as well as an average value for all samples available from each volcanic edifice. These average fractionation factors of 1.2–4.8 for the tephras and 0.7–3.8 for the edifices allow us to calculate fractionated cumulate masses from erupted magma masses for differentiation to >50 wt% SiO_2, which is a minimum estimate because we ignore the significant cumulate mass produced during fractionation from primitive compositions which, however, are not easily determined.

[45] The resulting total magma masses produced vary greatly between volcanoes, which reflects different modes of eruption and volcano ages. Edifice ages range up to 600 ka (Table 2) while the tephras we have studied cover the last 200 ka (except Tiribi Tuff at 320 ka). The tephra ages are well known but many of the edifice ages are not well constrained. We follow *Carr et al.* [2007b] in using 600 ka and 350 ka ages of undated volcanoes in Costa Rica and Nicaragua, respectively. Unpublished age data available to the Servicio Nacional de Estudios Territoriales (SNET) suggest 230 ka as a reasonable maximum age of undated volcanoes in El Salvador (C. Pullinger, SNET, personal communication, 2007). For Guatemala, we make the conservative assumption that undated volcano ages are equal to the oldest age yet determined (240 ka at Agua volcano [*Wundermann*, 1982]).

[46] Dividing the magma mass produced by each volcano by its lifetime yields long-term average magma fluxes. Figure 6 compares flux values obtained from edifice volumes alone, from combining edifice and tephra volumes, and from in-

Table 2. Summary of Ages, Edifice Volumes, and Tephra Volumes as Well as Respective Extrusive Masses and Calculated Fluxes Along the Central American Volcanic Arc[a]

Number	Volcanoes	Oldest Age at Complex, years	Age Ref.	Oldest Tephra at Complex, years	Age Ref.	Distance Along Arc, km	Edifice Volume, km^3	Edifice Magma Mass, kg	Magma flux 1, g/s	K_2O/K_2O_{50}	Magma Flux 2, g/s	Tephra Magma Mass, kg	Magma Flux 3, g/s	K_2O/K_2O_{50}	Magma Flux 4, g/s	Magma Flux 1+3, g/s	Magma Flux 2+4, g/s
								Guatemala									
1	Tacana	40,000	GP			22.3	20	5.60E+13	44,363	3.00	133,088					44,363	133,088
2	Tajumulco	240,000	X			46.7	45	1.26E+14	16,636	3.10	51,572					16,636	51,572
3	Cicabál	240,000	X			82.7	12	3.36E+13	4,436	2.30	10,203					4,436	10,203
4	Siete Orejas	240,000	X			84.7	40	1.12E+14	14,788	2.90	42,884					14,788	42,884
5	Cerro Que	240,000	X			94.8	5	1.40E+13	1,848	3.20	5,915					1,848	5,915
6	Santa Maria	240,000	X	140,000	R1	93.9	20	5.60E+13	7,394	2.40	17,745	1.96E+13	4,425	3.86	17,080	11,819	34,825
7	San Pedro	84,000	N			125.5	27	7.56E+13	28,519	2.30	65,594					28,519	65,594
8	Tolimán	84,000	N			135.3	18	5.04E+13	19,013	2.40	45,630					19,013	45,630
9	Atitlán	240,000	X	160,000	R1	137.1	33	9.24E+13	12,200	1.80	21,960	4.70E+14	93,161	4.83	449,966	105,360	471,925
10	Acatenango	230,000	V			169.2	62	1.74E+14	23,917	2.40	57,402					23,917	57,402
11	Fuego	100,000	MR			170.1	73	2.04E+14	64,770	1.40	90,677					64,770	90,677
12	Agua	240,000	W			183.0	68	1.90E+14	25,139	2.30	57,819					25,139	57,819
13	Pacaya	191,000	W			201.6	17	4.76E+13	7,897	1.50	11,846					7,897	11,846
14	Amatitlán			191,000	R1	205.0						1.71E+14	28,450	4.02	114,368	28,450	114,368
15	Tecuamburo	100,000	C2			231.0	39	1.09E+14	34,603	1.80	62,285					34,603	62,285
16	Moyuta	100,000	C2			266.5	15	4.20E+13	13,309	2.30	30,610					13,309	30,610
17	Ayarza			30,000	C2, PR	260.0						1.73E+13	18,305	4.50	82,374	18,305	82,374
								El Salvador									
18	Apaneca	230,000	P			304.5	125	3.50E+14	48,220	1.60	77,153					48,220	77,153
19	San Mareclino	230,000	P			318.0	1	2.80E+12	386	1.90	733					386	733
20	Santa Ana	230,000	P	80,000	CEL	319.4	220	6.16E+14	84,868	2.00	169,736	8.00E+11	317	4.50	1,426	85,185	171,162
21	Conejo	230,000	P			320.0	1	2.80E+12	386	1.80	694					386	694
22	Cerro Verde	230,000	P			321.1	2	5.60E+12	772	1.90	1,466					772	1,466
23	Izalco	300	R2			321.2	1	2.80E+12	295,752	1.65	487,990					295,752	487,990
24	Coatepeque		80,000	CEL	330.0						3.63E+13	14,376	4.02	57,793	14,376	57,793	
25	San Salvador	100,000	CEL	30,000	P	358.0	63	1.76E+14	55,897	2.00	111,794	3.24E+12	3,422	4.30	14,716	59,319	126,510
26	Ilopango	230,000	P	40,000	K	383.0	30	8.40E+13	11,573	3.80	43,977	9.31E+13	73,755	3.81	281,005	85,327	324,982
27	San Vincente	230,000	P			404.1	60	1.68E+14	23,146	2.30	53,235					23,146	53,235
28	Berlin	230,000	P	80,000	CEL	440.0	60	1.68E+14	23,146	1.60	37,033	9.29E+13	36,815	3.10	114,126	59,961	151,159
29	Tigre	150,000	CEL			441.0	20	5.60E+13	11,830	1.60	18,928					11,830	18,928
30	Taburete	230,000	P			442.7	8	2.24E+13	3,086	1.60	4,938					3,086	4,938
31	Tecapa	75,000	CEL			443.0	65	1.82E+14	76,895	1.60	123,033					76,895	123,033
32	Usulatán	220,000	CEL			449.8	15	4.20E+13	6,049	1.20	7,259					6,049	7,259
33	Chinameca	230,000	P			460.0	10	2.80E+13	3,858	1.50	5,786					3,858	5,786
34	Pacayal	230,000	P	80,000	CEL	462.0	1	2.80E+12	386	1.20	463	3.40E+13	13,479	3.10	41,785	13,865	42,248
35	San Miguel	230,000	P	80,000	CEL	467.0	58	1.62E+14	22,374	1.30	29,087	1.20E+13	4,753	2.00	9,506	27,127	38,593

Table 2. (continued)

Number	Volcanoes	Oldest Age at Complex, years	Age Ref.	Oldest Tephra at Complex, years	Age Ref.	Distance Along Arc, km	Edifice Volume, km^3	Edifice Magma Mass, kg	Magma flux 1, g/s	K_2O/K_2O_{50}	Magma Flux 2, g/s	Tephra Magma Mass, kg	Magma Flux 3, g/s	K_2O/K_2O_{50}	Magma Flux 4, g/s	Magma Flux 1+3, g/s	Magma Flux 2+4, g/s
36	Conchagua	230,000	P			514.0	27	7.56E+13	10,416	1.50	15,623					10,416	15,623
37	Conchaguita	230,000	P			524.0	1	2.80E+12	386	1.30	501					386	501
38	Meanguera	230,000	P			531.0	3	8.40E+12	1,157	1.30	1,504					1,157	1,504
								Nicaragua									
39	Cosigüina	350,000	C1	25,000	K	556.0	33	9.24E+13	8,366	2.30	19,241	2.45E+13	31,117	2.32	72,192	39,483	91,432
40	San Cristobal	350,000	C1			624.0	110	3.08E+14	27,885	1.50	41,828					27,885	41,828
41	Casita	350,000	C1			627.0	45	1.26E+14	11,408	1.50	17,111					11,408	17,111
42	Telica	350,000	C1			644.0	30	8.40E+13	7,605	1.30	9,887					7,605	9,887
43	St. Clara	350,000	C1			648.0	2	5.60E+12	507	1.30	659					507	659
44	Rota	350,000	C1			655.0	12	3.36E+13	3,042	1.40	4,259					3,042	4,259
45	Malpaisillo		300,000	vWdV	660.0						3.00E+13	3,169	3.42	10,837	3,169	10,837	
46	Cerro Negro	150	MW			663.0	0.2	5.60E+11	118,301	1.00	118,301					118,301	118,301
47	Las Pilas	350,000	C1			665.0	28	7.84E+13	7,098	2.00	14,196					7,098	14,196
48	El Hoyo	350,000	C1			667.0	14	3.92E+13	3,549	1.90	6,743					3,549	6,743
49	Momotombo	350,000	C1			683.3	18	5.04E+13	4,563	1.60	7,301					4,563	7,301
50	Apoyeque	350,000	C1	17,000	K	711.2	6	1.68E+13	1,521	3.60	5,476	3.03E+13	56,421	3.65	205,937	57,942	211,412
51	Nejapa	30,000	F			720.0	3	8.40E+12	8,873	1.40	12,422					8,873	12,422
52	Masaya	350,000	C1	60,000	K	742.7	178	4.98E+14	45,123	1.00	45,123	3.48E+13	18,383	1.15	21,141	63,507	66,264
53	Apoyo	90,000	S	25,000	K	754.8	10	2.80E+13	9,858	1.40	13,802	7.82E+13	99,155	3.52	349,027	109,014	362,829
54	Mombacho	350,000	C1			762.2	20	5.60E+13	5,070	0.70	3,549					5,070	3,549
55	Granada	350,000	C1			766.4	3	8.40E+12	761	2.60	1,977					761	1,977
56	Zapatera	350,000	C1			784.8	5	1.40E+13	1,268	1.80	2,282					1,268	2,282
57	Concepción	350,000	C1	19,000	K	816.9	19	5.32E+13	4,817	1.90	9,151	7.34E+12	12,248	3.10	37,968	17,064	47,120
58	Maderas	350,000	C1			834.0	22	6.16E+13	5,577	1.80	10,039					5,577	10,039
								Costa Rica									
59	Orosi	600,000	C1			861.5	75	2.10E+14	11,091	1.00	11,091					11,091	11,091
60	Cacao					863.0											
61	Rincón de la Vieja	600,000	C1	30,000	Ch	882.3	102	2.86E+14	15,083	2.10	31,675	5.00E+11	528	2.50	1,320	15,611	32,995
62	Miravaelles	600,000	C1			903.9	60	1.68E+14	8,873	2.10	18,632					8,873	18,632
63	Tenorio	600,000	C1			920.4	49	1.37E+14	7,246	2.10	15,216					7,246	15,216
64	Arenal	600,000	C1	30,000	Ch	958.3	11	3.08E+13	1,627	1.80	2,928	2.00E+12	2,113	2.50	5,281	3,739	8,209
65	Alto Palomo		550,000	Vl	980.0						1.81E+14	10,417	3.00	31,252	10,417	31,252	

Table 2. (continued)

Number	Volcanoes	Oldest Age at Complex, years	Age Ref.	Oldest Tephra at Complex, years	Age Ref.	Distance Along Arc, km	Edifice Volume, km^3	Edifice Magma Mass, kg	Magma flux 1, g/s	K_2O/K_2O_{50}	Magma Flux 2, g/s	Tephra Magma Mass, kg	Magma Flux 3, g/s	K_2O/K_2O_{50}	Magma Flux 4, g/s	Magma Flux 1+3, g/s	Magma Flux 2+4, g/s
66	Platanar	600,000	C1			1001.7	84	2.35E+14	12,422	2.40	29,812					12,422	29,812
67	Poas	600,000	C1	30,000	Ch	1021.0	97	2.72E+14	14,344	1.90	27,254	2.00E+12	2,113	3.00	6,338	16,456	33,591
68	Tiribi			320,000	Pz	1030.0						4.97E+13	4,917	3.30	16,225	4,917	16,225
69	Barva	600,000	C1	30,000	Ch	1037.0	197	5.52E+14	29,132	1.70	49,524	1.20E+12	1,268	3.00	3,803	30,399	53,326
70	Irazú	600,000	C1	30,000	Ch	1067.0	242	6.78E+14	35,786	1.70	60,836	1.20E+12	1,268	2.80	3,549	37,053	64,385
71	Turialba	600,000	C1			1072.0	87	2.44E+14	12,865	2.50	32,163					12,865	32,163

[a] Age data from C1, *Carr et al.* [2007b]; C2, *Cameron et al.* [2002]; CEL, *CEL* [1992, 1995]; Ch, *Chiesa* [1991], *Chiesa et al.* [1992]; F, *Freundt et al.* [2006]; GP, *Garcia-Palomo et al.* [2006]; K, *Kutterolf et al.* [2008]; MR, *Martin and Rose* [1981]; MW, *McKnight and Williams* [1997]; N, *Newhall* [1987]; P, C. Pullinger (personal communication, 2007), best estimate; PR, *Petersen and Rose* [1985]; Pz, *Pérez et al.* [2006]; R1, *Rose et al.* [1999]; R2, *Rose* [1987]; S, *Sussman* [1985]; V, *Vallance et al.* [2001]; Vl, *Vogel et al.* [2004]; vWdV, *Van Wyk de Vries* [1993]; W, *Wundermann* [1982]; X, we use the oldest age for Agua (W) also for other volcanoes where no age data are available. Edifice volumes from *Carr et al.* [2007b] for Costa Rica and Nicaragua and *Carr et al.* [2003] for El Salvador and Guatemala. K_2O/K_2O_{50} is average fractionation factor used to calculate mass of fractionated cumulates. K_2O is actual content in the rocks; K_2O_{50} is K_2O content at 50% SiO_2. Compositional data for edifices from *Carr et al.* [2003] and *Patino et al.* [2000]. Compositional data for tephras from *Kutterolf et al.* [2008] and auxiliary material Table S1. Magma flux 1, flux based on edifice volumes; magma flux 2, flux based on edifice volumes and including fractionated cumulates; magma flux 3, flux based on tephra volumes; magma flux 4, flux based on tephra volumes and including fractionated cumulates; magma flux 1 + 3, total eruptive magma flux; magma flux 2 + 4, total magma flux at each volcano.

cluding masses of fractionated cumulates. The along-arc variation is highly irregular but peak magma fluxes from volcanoes that stand out by their high productivity increase northward along the CAVA. Overall, magma fluxes are higher in El Salvador than in Nicaragua and Costa Rica.

[47] The sum of total magma fluxes (including cumulates) for the entire 1100 km length of the CAVA studied is $4.5*10^6$ g/s, which divided by the length gives an average flux per unit arc length of 4.2 g/s/m. The long-term average eruptive magma fluxes of CAVA volcanoes range across 400–296,000 g/s which agrees with global estimates for oceanic arcs (8,200–667,000 g/s; avg. 177,000 g/s) as determined by *White et al.* [2006] but is lower than respective values for continental arcs (940–6,344,000 g/s; avg. 481,000 g/s). *Wadge et al.* [2006] determined a magma flux of about 1,400,000 g/s for Arenal volcano, Costa Rica, from the volumes of lava extruded from 1980 until 2004. Our value for the long-term (600 ka) erupted magma flux of Arenal is 3,739 g/s. This example emphasizes the temporal variability of magma fluxes at the volcanoes. While short-term measurements are important for topics such as hazard

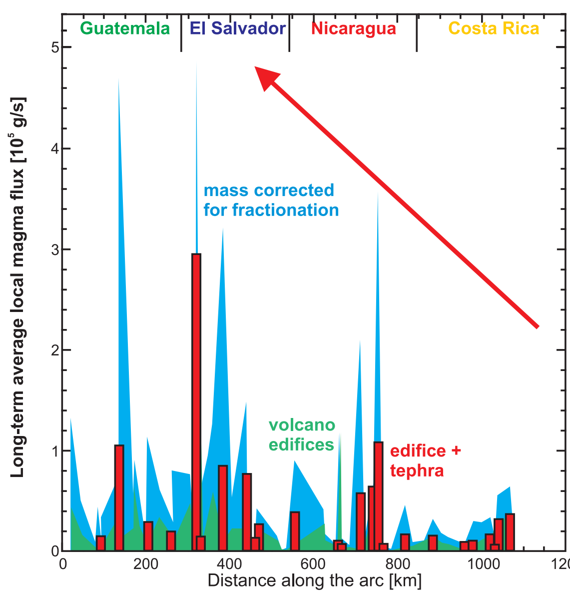

Figure 6. Magma mass fluxes from CAVA volcanoes averaged over volcano age and based on edifice volumes (green) and on edifice plus tephra volumes (red). Extrusive mass fluxes (derived from edifice plus tephra volumes, in red) are compared with total magma fluxes including fractionated cumulate masses trapped in the crust (for differentiation above 50 wt% SiO_2, in blue). The red arrow shows the increase of peak total magma fluxes from Costa Rica to Guatemala.

assessment, the long-term behavior is the more important in studying how arc volcanism relates to subduction processes. The long-term magma fluxes determined here are a prerequisite to determine elemental fluxes through the volcanic arc such as those of H_2O and other volatiles which, in turn, can be compared with subduction input fluxes to better understand the transfer processes operating in the subduction zone.

[48] However, the magma mass fluxes we have determined suffer from a number of uncertainties. The ages of some of the CAVA volcanoes are only poorly constrained. The known tephra record does not cover the entire lifetime of some volcanoes because older tephras or poorly exposed or preserved. More important, however, are two other factors. First, the total magma flux should also include intrusive magmas that never reached the surface. Intrusive bodies may eventually be visualized by geophysical methods but still their ages and compositions would remain unknown. Surface deformation measured by satellite radar interferometry can provide information on crustal inflation by intruding magmas and allows to determine magma flow rates [*Pritchard and Simons*, 2004] but such momentary data may not be representative of the long-term arc evolution as indicated by the Arenal example mentioned above. If there is some constant ratio between extrusive and intrusive magma flux, the absolute values but not the pattern of along-arc variation shown in Figure 6 would change. The second factor not accounted for is erosion which can be substantial during volcano lifetimes of order 10^5 years. Volcaniclastic detritus eroded from the CAVA is ultimately delivered into the Pacific Ocean. From a reconnaissance study of forearc sediments sampled in our gravity cores offshore Nicaragua we estimate that a minimum of 30% should be added to the long-term magma fluxes to account for the erosive losses. However, more detailed work on the marine and terrestrial volcaniclastic sediments is needed to really quantify erosion rates and their variation along the CAVA which rises to greater elevations above sea level northward.

7. Summary

[49] Using the correlations of marine tephras to onshore eruptions from part1, we have constructed isopach maps of the widespread tephras produced at the CAVA during the last 200 ka. The offshore thickness data allowed us to determine more realistic volumes of these correlated tephras than was possible from on-land exposures. In Central America, where the volcanic arc lies only a few tens of kilometers upwind from the Pacific coast, the tephra volume emplaced in the ocean, on average, makes up 60% of the total erupted volume which is still a minimum estimate since we only considered isopachs of $\geq$1 cm thickness. The largest single eruptions, such as those of the Los Chocoyos ash and L-Tephra in Guatemala, occurred at the northern part of the CAVA but are not as frequent as the eruptions from Nicaragua and Southern Salvador with an overall smaller magnitude (Figure 4). This is also reflected in the greater thickness and coarser grain size of the Pacific ash layers offshore Guatemala and Northern El Salvador compared to those near Nicaragua and Costa Rica.

[50] We have integrated tephra volumes and published volumes of the volcanic edifices, and we have calculated the associated masses of fractionated cumulates from chemical compositions to determine the total magma mass produced by each CAVA volcano during its lifetime. Division by volcano ages yielded the long-term average magma flux at each volcano. The resulting data show that, averaged over the CAVA, highly explosive eruptions generating widespread tephras account for at least 65% of the total magma output. Magma fluxes of neighboring volcanoes are often vastly different and peak fluxes increase northward along the CAVA. Compared to estimates of global average volcanic magma fluxes, the long-term fluxes of CAVA volcanoes reach comparable magma fluxes regarding oceanic island arcs and slightly lower values for continental arcs. The magma flux values we have compiled here form a useful basis to calculate elemental fluxes of volcanic output as an important aspect in the overall flux budget of the Central American subduction zone.

Acknowledgments

[51] We gratefully acknowledge the support during field work by the local geological surveys: SNET in El Salvador, INETER in Nicaragua, and INSIVUMEH in Guatemala. We particularly appreciate the permission to use unpublished thickness data by Carlos Pullinger, Dolores Ferres, Walther Hernadez, and Heidi Wehrmann. Wendy Peréz acknowledges a Ph.D. stipend by the Deutscher Akademischer Austauschdienst (DAAD). Many thanks also to all members of the scientific parties of the R/V *METEOR* and R/V *SONNE* cruises for the assistance in drilling, logging, and sampling the gravity cores. R/V *METEOR* and R/V *SONNE* cruises were funded by the Deutsche Forschungsgemeinschaft (DFG). We also appreciate the helpful comments and suggestions of Vincent Salters, Stephen Blake, Mike Carr, Phil Shane, and Tom Vogel, who

reviewed this paper. This publication is contribution 98 of the Sonderforschungsbereich 574 "Volatiles and Fluids in Subduction Zones" at Kiel University.

References

Barckhausen, U., C. R. Ranero, R. von Huene, S. Cande, and H. Roeser (2001), Revised tectonic boundaries in the Cocos Plate off Costa Rica: Implications for the segmentation of the convergent margin and for plate tectonic models, *J. Geophys. Res.*, *106*(19), 207–220.

Bice, D. C. (1980), Tephrostratigraphy and physical aspects of recent volcanism near Managua, Nicaragua, 422 pp., Ph.D. thesis, Univ. of Calf., Berkeley, Berkeley.

Bice, D. C. (1985), Quaternary volcanic stratigraphy of Managua, Nicaragua: Correlation and source assignment for multiple overlapping plinian deposits, *Geol. Soc. Am. Bull.*, *96*, 553–566.

Borgia, A., and B. van Wyk de Vries (2003), The volcano-tectonic evolution of Concepción, Nicaragua, *Bull. Volcanol.*, *65*, 248–266.

Bowles, F. A., R. N. Jack, and I. S.E. Carmichael (1973), Investigation of deep-sea volcanic ash layers from equatorial Pacific cores, *Geol. Soc. Am. Bull.*, *84*, 2371–2388.

Cameron, B. I., et al. (2002), Flux versus decompression melting at stratovolcanoes in southeastern Guatemala., *J. Volcanol. Geotherm. Res.*, *119*, 21–50.

Carr, M., M. D. Feigenson, L. C. Patino, and J. A. Walker (2003), Volcanism and geochemistry in Central America: Progress and problems, in *Inside the Subduction Factory*, *Geophys. Monogr. Ser.*, vol. 138, edited by J. Eiler, pp. 153–174, AGU, Washington, D. C.

Carr, M. J. (1984), Symmetrical and segmented variation of physical and geochemical characteristics of the Central American Volcanic Front, *J. Volcanol. Geotherm. Res.*, *20*, 231–252.

Carr, M. J., M. D. Feigensohn, and E. A. Benett (1990), Incompatible element and isotopic evidence for tectonic control of source mixing and melt extraction along the Central American arc, *Contrib. Mineral. Petrol.*, *105*, 369–380.

Carr, M. J., L. C. Patino, and M. D. Feigenson (2007a), Petrology and geochemistry of lavas, in *Central America—Geology, Resources and Hazards*, vol. 2, edited by J. Buntschuh and G. E. Alvarado, pp. 565–590, A. A. Balkema, Rotterdam, Netherlands.

Carr, M. J., I. Saginor, G. E. Alvarado, L. L. Bolge, F. N. Lindsay, K. Milidakis, B. D. Turrin, M. D. Feigenson, and C. C. Swisher III (2007b), Element fluxes from the volcanic front of Nicaragua and Costa Rica, *Geochem. Geophys. Geosyst.*, *8*, Q06001, doi:10.1029/2006GC001396.

Chiesa, S. (1991), El Flujo de Pomez biotitica del Rio Liberia (Guanacaste) Costa Rica, America Central, *Rev. Geol. Am. Cent.*, *13*, 73–84.

Chiesa, S., G. Civelli, P.-Y. Gillot, O. Mora, and G. E. Alvarado (1992), Rocas piroclásticas asociadas con La Formación de la Caldera de Guayabo, Cordillera de Guanacaste, Costa Rica, *Rev. Geol. Am. Cent.*, *14*, 59–75.

Commision Ejecutiva Hidroelectrica del Rio Lempa (CEL) (1992), Desarrollo de los Recursos Geotermicos del Area Centro-Occidental de El Salvador, Prefactibilidad Geotermica del Area de Coatepeque, Reconocimiento Geotermico, San Salvador.

CEL (1995), Prestacion de Servicios de Consultoria para desarrollar Estudios Geocientificos Complementarios en el Campo Geotermico Berlin-Partida 4: Estudio Geovulcanica, y Recursos Geotermicos del Area Berlin-Chinameca, Prefactibilidad Geotermica del Area de Coatepeque, Reconocimiento Geotermico, Informe Definitivo, internal report, San Salvador.

Cruciani, C., E. Carminati, and C. Doglioni (2005), Slab dip vs. lithosphere age: No direct function, *Earth Planet. Sci. Lett.*, *238*, 298–310.

DeMets, C. (2001), A new estimate for present-day Cocos-Caribbean plate motion: Implications for slip along the Central American volcanic arc, *Geophys. Res. Lett.*, *28*, 4043–4046.

Drexler, J. W., W. I. Rose, Jr., R. S.J. Sparks, and M. T. Ledbetter (1980), The Los Chocoyos Ash, Guatemala: A major stratigraphic marker in Middle America and in the three ocean basins, *Quat. Res.*, *13*, 327–345.

Dull, R. A., J. R. Southon, and P. D. Sheets (2001), Volcanism, ecology and culture: A reassessment of the Volcán Ilopango TBJ eruption in the Southern Maya Realm, *Latin Am. Antiquity*, *12*(1), 25–44.

Ehrenborg, J. (1996), A new stratigraphy for the Tertiary volcanic rocks of the Nicaraguan highland, *Geol. Soc. Am. Bull.*, *108*, 830–842.

Feigenson, M. D., and M. J. Carr (1986), Positively correlated Nd and Sr isotope ratios of lavas from the Central American volcanic front, *Geology*, *14*, 79–82.

Feigenson, M. D., M. J. Carr, S. V. Maharaj, S. Juliano, and L. L. Bolge (2004), Lead isotope composition of Central American volcanoes: Influence of the Galapagos plume, *Geochem. Geophys. Geosyst.*, *5*, Q06001, doi:10.1029/2003GC000621.

Fierstein, J., and M. Nathenson (1992), Another look at the calculation of fallout tephra volumes, *Bull. Volcanol.*, *54*, 156–167.

Freundt, A., S. Kutterolf, H. U. Schmincke, T. H. Hansteen, H. Wehrmann, W. Perez, W. Strauch, and M. Navarro (2006), Volcanic hazards in Nicaragua: Past, present, and future, in *Volcanic Hazards in Central America*, edited by W. I. Rose et al., *Spec. Pap. Geol. Soc. Am.*, *412*, 141–165.

Garcia-Palomo, A., J. L. Macias, J. L. Arce, J. C. Mora, S. Hughes, R. Saucedo, J. M. Espindola, R. Escobar, and P. Layer (2006), Geological evolution of the Tacaná Volcanic Complex, México-Guatemala, in *Volcanic Hazards in Central America*, edited by W. I. Rose et al., *Spec. Pap. Geol. Soc. Am.*, *412*, 39–58.

Grevemeyer, I., N. Kaul, J. L. Diaz-Naveas, H. W. Villinger, C. R. Ranero, and C. Reichert (2005), Heat flow and bending-related faulting at subduction trenches: Case studies offshore of Nicaragua and central Chile, *Earth. Planet. Sci. Lett.*, *236*, 238–248.

Hart, W. J. E. (1983), Classic to postclassic tephra layers exposed in archeological sites, eastern Zapotitán Valley, in *Archeology and Volcanism in Central America—The Zapotitán Valley of El Salvador*, edited by P. D. Sheets, pp. 44–51, Univ. of Tex. Press, Austin.

Hart, W. J. E., and V. Steen-McIntyre (1983), Terra Blanca Joven tephra from the AD 260 eruption of Ilopongo Caldera, in *Archeology and Volcanism in Central America—The Zapotitán Valley of El Salvador*, edited by P. D. Sheets, pp. 15–34, Univ. of Tex. Press, Austin.

Hoernle, K., P. van den Bogaard, R. Werner, B. Lissinna, G. E. Alvarado, and C.-D. Garbe-Schönberg (2002), Missing history (16–71 Ma) of the Galapagos hotspot: Implications for the tectonic and biological evolution of the Americas, *Geology*, *30*(9), 795–798.

Koch, A. J., and H. McLean (1975), Pleistocene tephra and ash-flow deposits in the volcanic highlands of Guatemala, *Geol. Soc. Am. Bull.*, *86*, 529–541.

Kutterolf, S., U. Schacht, H. Wehrmann, A. Freundt, and T. Mörz (2007a), Onshore to offshore tephrostratigraphy and marine ash layer diagenesis in Central America, in *Central America—Geology, Resources and Hazards*, vol. 2, edited by J. Buntschuh and G. E. Alvarado, pp. 395–423, A. A. Balkema, Lisse, Netherlands.

Kutterolf, S., A. Freundt, W. Peréz, H. Wehrmann, and H.-U. Schmincke (2007b), Late Pleistocene to Holocene temporal succession and magnitudes of highly-explosive volcanic eruptions in west-central Nicaragua, *J. Volcanol. Geotherm. Res.*, *163*, 55–82.

Kutterolf, S., A. Freundt, W. Peréz, T. Mörz, U. Schacht, H. Wehrmann, and H.-U. Schmincke (2008), Pacific offshore record of plinian arc volcanism in Central America: 1. Along-arc correlations, *Geochem. Geophys. Geosyst.*, doi:10.1029/2007GC001631, in press.

Ledbetter, M. T. (1985), Tephrochronology of marine tephra adjacent to Central America, *Geol. Soc. Am. Bull.*, *96*, 77–82.

Mann, C. P., J. Stix, J. W. Vallance, and M. Richer (2004), Subaqueous intracaldera volcanism, Ilopango Caldera, El Salvador, Central America, in *Natural Hazards in El Salvador*, edited by W. I. Rose et al., *Spec. Pap. Geol. Soc. Am.*, *375,* 159–174.

Martin, D. P., and W. I. Rose (1981), Behavior patterns of Fuego Volcano, Guatemala, *J. Volcanol. Geotherm. Res.*, *10*, 67–81.

McKnight, S. B., and S. N. Williams (1997), Old cinder cone or young composite volcano?: The nature of Cerro Negro,-Nicaragua, *Geology*, *25*, 339–342.

Newhall, C. G. (1987), Geology of the Lake Atitlàn region, western Guatemala, *J. Volcanol. Geotherm. Res.*, *33*, 23–55.

Patino, L. C., M. Carr, and M. D. Feigenson (1997), Cross-arc geochemical variations in volcanic fields in Honduras C. A.: Progressive changes in source with distance from the volcanic front, *Contrib. Mineral. Petrol.*, *129*, 341–351.

Patino, L. C., M. Carr, and M. D. Feigenson (2000), Local and regional variations in Central American arc lavas controlled by variations in subducted sediment input, *Contrib. Mineral. Petrol.*, *138*, 256–283.

Pérez, W., and A. Freundt (2006), The youngest highly explosive basaltic eruptions from Masaya Caldera (Nicaragua): Stratigraphy and hazard assessment, in *Volcanic Hazards in Central America*, edited by W. I. Rose et al., *Spec. Pap. Geol. Soc. Am.*, *412*, 189–207.

Pérez, W., G. E. Alvarado, and P. B. Gans (2006), The 322 ka Tiribi Tuff: Stratigraphy, geochronology and mechanisms of deposition of the largest and most recent ignimbrite in the Valle Central, Costa Rica, *Bull. Volcanol.*, *69*, 25–40.

Peterson, P. S., and W. I. Rose (1985), Explosive eruptions of the Ayarza Calderas, southeastern Guatemala, *J. Volcanol. Geotherm. Res.*, *25*, 289–307.

Pouclet, A., J.-P. Cadet, F. K., and J. Bourgois (1985), Ash layers from Deep Sea Drilling Project Leg 84: Middle America Trench Transect, *Initial Rep. Deep Sea Drill. Proj.*, *84*, 609–618.

Pritchard, M. E., and M. Simons (2004), Surveying volcanic arcs with satellite radar interferometry: The central Andes, Kamchatka, and beyond, *GSA Today*, *14*, 4–11.

Protti, M., F. Gundel, and K. McNally (1995), Correlation between the age of the subducting Cocos plate and the geometry of the Wadati-Benioff zone under Nicaragua and Costa Rica, in *Geologic and Tectonic Development of the Caribbean Plate Boundary in Southern Central America*, edited by P. Mann, *Spec. Pap. Geol. Soc. Am.*, *295*, 309–326.

Pullinger, C. R. (1998), Evolution of the Santa Ana volcanic complex, El Salvador, 145 pp., M. S. thesis, Mich. Technol. Univ., Houghton.

Pyle, D. M. (1989), The thickness, volume and grain size of tephra fall deposits, *Bull. Volcanol.*, *51*, 1–15.

Rabek, K., M. T. Ledbetter, and D. F. Williams (1985), Tephrochronology of the western Gulf of Mexico, *Quat. Res.*, *23*, 403–416.

Ranero, C. R., J. Phipps Morgan, K. McIntosh, and C. Reichert (2003), Bending-related faulting and mantle serpentinization at the Middle America trench, *Nature*, *425*, 367–373.

Ranero, C. R., A. Villaseñor, J. Phipps Morgan, and W. Weinrebe (2005), Relationship between bend-faulting at trenches and intermediate-depth seismicity, *Geochem. Geophys. Geosyst.*, *6*, Q12002, doi:10.1029/2005GC000997.

Rose, W. I. (1987), Santa Maria, Guatemala: Bimodal soda-rich calc-alkalic stratovolcano, *J. Volcanol. Geotherm. Res.*, *33*, 109–129.

Rose, W. I., C. G. Newhall, T. J. Bornhorst, and S. Self (1987), Quaternary silicic pyroclastic deposits of Atitlàn Caldera, Guatemala, *J. Volcanol. Geotherm. Res.*, *33*, 57–80.

Rose, W. I., F. M. Conway, C. R. Pullinger, A. Deino, and K. McIntosh (1999), An improved age framework for late Quaternary silicic eruptions in northern Central America, *Bull. Volcanol.*, *61*, 106–120.

Rüpke, L. H., J. P. Morgan, M. Hort, and J. A.D. Connolly (2002), Are the regional variations in Central American arc lavas due to differing basaltic versus peridotitic slab sources of fluids?, *Geology*, *30*, 1035–1038.

Scott, W., C. Gardner, A. Alverez, and G. Devoli (2006), A. D. 1835 eruption of Volcán Cosigüina, Nicaragua: A guide for assessing hazards, in *Volcanic Hazards in Central America*, edited by W. I. Rose et al., *Spec. Pap. Geol. Soc. Am.*, *412*, 167–187.

Self, S., M. R. Rampino, and M. Carr (1989), A reappraisal of the 1835 eruption of Coseguina and its atmospheric impact, *Bull. Volcanol.*, *52*, 57–65.

Sussman, D. (1985), Apoyo Caldera, Nicaragua: A major Quaternary silicic eruptive center, *J. Volcanol. Geotherm. Res.*, *24*, 249–282.

Syracuse, E. M., and G. A. Abers (2006), Global compilation of variations in slab depth beneath arc volcanoes and implications, *Geochem. Geophys. Geosyst.*, *7*, Q05017, doi:10.1029/2005GC001045.

Vallance, J. W., S. P. Schilling, O. Matías, W. I. Rose, and M. M. Howell (2001), Volcano Hazards at Fuego and Acatenango, Guatemala, *U.S. Geol. Surv. Open File*, *01-431*.

Van Wyk de Vries, B. (1993), Tectonics and magma evolution of Nicaraguan volcanic systems, doctoral thesis, 328 pp., Open Univ., Milton Keynes, U. K.

Vogel, T. A., L. C. Patino, G. E. Alvarado, and P. B. Gans (2004), Silicic ignimbrites within the Costa Rican volcanic front: Evidence for the formation of continental crust, *Earth. Planet. Sci. Lett.*, *226*, 149–159.

Wadge, G., D. Oramas Dorta, and P. D. Cole (2006), The magma budget of Volcan Arenal, Costa Rica, from 1980 to 2004, *J. Volcanol. Geotherm. Res.*, *157*, 60–74.

Wehrmann, H., C. Bonadonna, A. Freundt, B. F. Houghton, and S. Kutterolf (2006), Fontana Tephra: A basaltic plinian eruption in Nicaragua, in *Volcanic Hazards in Central America*, edited by W. I. Rose et al., *Spec. Pap. Geol. Soc. Am.*, *412*, 209–223.

White, S. M., J. A. Crisp, and F. J. Spera (2006), Long-term volumetric eruption rates and magma budgets, *Geochem. Geophys. Geosyst.*, *7*, Q03010, doi:10.1029/2005GC001002.

Williams, H. (1952), The great eruption of Cosequina, Nicaragua, in 1835, with notes on the Nicaraguan volcanic chain, *Univ. Calif. Publ. Geol. Sci.*, *29*, 21–45.

Williams, S. N. (1993), Geology and eruptive mechanisms of Masaya Caldera Complex, Nicaragua, 169 pp., Ph.D. thesis, Dartmouth Coll., Hanover, N. H.

Wundermann, R. L. (1982), Amatitlàn, an active resurgent caldera immediately south of Guatemala City, Guatemala, 192 pp., M. S. thesis, Mich. Technol. Univ., Houghton.

Wundermann, R. L., and W. I. Rose (1984), Amatitlán, an actively resurging caldera 10 km south of Guatemala City, *J. Geophys. Res.*, *89*, 8525–8539.